Periodic forcing of spiral waves in excitable media

Rolf-Martin Mantel and Dwight Barkley
Mathematics Institute and Nonlinear Systems Laboratory, University of Warwick, Coventry CV4 7AL, United Kingdom
(Received 3 June 1996)

An analysis of periodically forced spiral waves in excitable media provides a simple explanation of the resonant drift dynamics and frequency entrainments observed both in laboratory experiments and in simulations of partial-differential equations. Forcing of both rigidly rotating and meandering spirals is considered. In the meandering case we predict the existence of different resonant drift states that could be detected in experiments. [S1063-651X(96)10411-6]

PACS number(s): 82.40.Ck

I. INTRODUCTION

The response of spiral waves in excitable media to homogeneous periodic forcing is of interest for a variety of reasons. First, as Figs. 1(a) and 1(b) illustrate, a drift in the location of a rotating spiral wave can be produced by periodically varying a system parameter at the spiral rotation frequency. This has been recognized as a possible means of low-voltage cardiac defibrillation [1–6]; the idea is essentially that with relatively weak periodic forcing one can induce rotating waves within a fibrillating heart to drift to a boundary (heart's surface) where they can no longer be sustained. A second reason for interest in this problem is that spiral waves occur in a variety of biological systems and these are often subjected to some form of external forcing, as, for example, might occur due to daily variations in sunlight, and it is important to understand the role such external driving can play in these systems. Finally, as shown in Figs. 1(c) and 1(d), when ''meandering'' waves in excitable media are periodically forced, they can exhibit complex motions, and it is desirable to have a simple mathematical description of these motions.

Our approach shall be to consider the periodic forcing of spiral waves from a dynamical-systems view point and to show that much of the spiral behavior can be deduced simply from the interaction of dynamics with system symmetries. We base our analysis on a system of ordinary differential equations described in Sec. II. This system has been shown to model well the dynamics of spiral waves, though it has not been obtained by rigorous reduction of a partial-differential equation model of excitable media.

We shall be particularly interested in the forcing of meandering spiral waves, i.e., the case where the unforced system has quasiperiodic waves. This interesting situation has received much attention recently in experiments and simulations [5,7–10], but it has not been given a proper theoretical footing. We show that many drifting states are possible in the meandering case and we predict some not previously seen in experiment.

We stress that while our focus is the periodic forcing of spiral waves in excitable media, our approach is general and hence our results on homogeneous, periodic forcing are fully applicable to any system exhibiting rotating waves in the presence of distance-preserving symmetries of the plane.

II. MODEL EQUATIONS

Our starting point is a system of ordinary differential equations (ODEs) describing the dynamics of periodic and meandering spiral waves in homogeneous, unbounded excitable media [12–14]:

$$\begin{aligned} \dot{p} &= s e^{i\phi}, \\ \dot{\phi} &= \omega, \\ \dot{s} &= s f(s^2, \omega^2), \\ \dot{\omega} &= \omega g(s^2, \omega^2), \end{aligned} \tag{1}$$

where p is complex and ϕ, s, and ω are real with $s \geq 0$. As the notation suggests, p is thought of as the position of the spiral tip and we write $p = x + iy$. Then s is the linear speed (scalar) and ω is the instantaneous rotational frequency of the spiral tip. The real-valued functions f and g are

$$\begin{aligned} f(s^2, \omega^2) &= -1/4 + \alpha_1 s^2 + (\alpha_2 / \gamma_0^2)\omega^2 - s^4, \\ g(s^2, \omega^2) &= s^2 - \omega^2/\gamma_0^2 - 1. \end{aligned} \tag{2}$$

Equations (1) and (2) have been derived from a symmetric bifurcation analysis of spiral dynamics [12–14], but here a slightly different form is used [15]. They are essentially the simplest system of ODEs that have the relevant symmetries for two-dimensional excitable media (namely, rotations, reflections, and translations) and have a supercritical Hopf bifurcation from rotating-wave solutions. Thus these equations can be thought of as a kind of normal form for spiral dynamics. While the equations have been obtained from an analysis of the transition from periodic to meandering spiral dynamics, they have been shown to describe qualitatively a wide range of behavior observed in homogeneous excitable media [14,16–18].

Consider the s-ω subsystem described by

$$\dot{s} = s f(s^2, \omega^2), \quad \dot{\omega} = \omega g(s^2, \omega^2). \tag{3}$$

It can be seen that the subsystem decouples in Eqs. (1) and that $\phi(t)$ and $p(t) = x(t) + iy(t)$ can be found by quadrature once $s(t)$ and $\omega(t)$ are known. Thus the dynamics of rotating and meandering spiral waves in homogeneous excitable media can be reduced to a simple two-variable ODE system

 © 1996 The American Physical Society

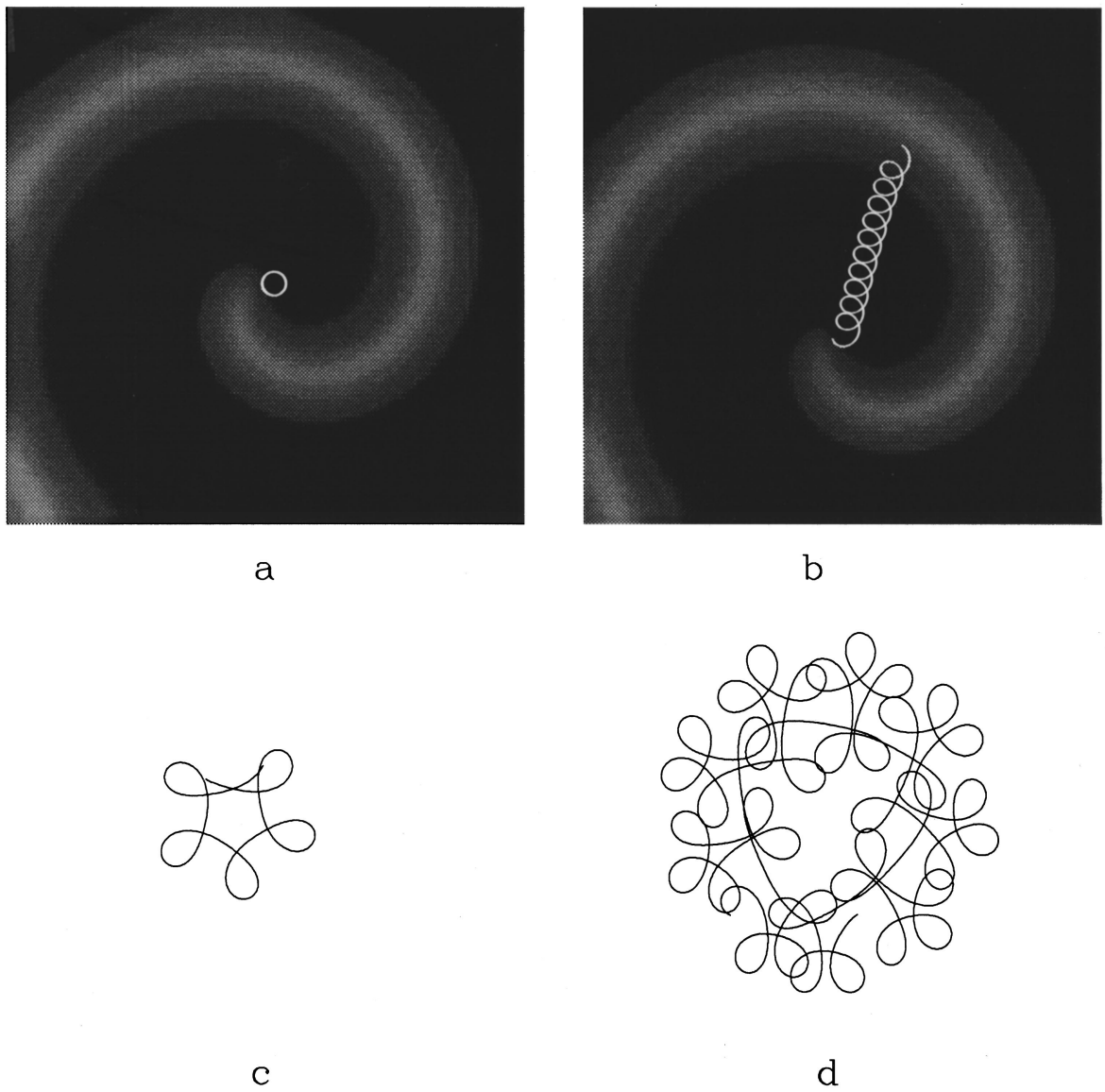

FIG. 1. Illustration of the effects of periodic forcing on the spiral-wave dynamics. (a) Periodically rotating solution in a reaction-diffusion model of homogeneous excitable media [11]. The gray scale shows values of the slow species and the white curve shows the path of the spiral tip. The model parameters are $a=0.8$, $b=0.05$, and $\epsilon=0.02$. (b) Same conditions as (a), except with spatially homogeneous forcing at the rotation frequency of the unforced spiral. The induced drift in the spiral location is from top to bottom in this case. Here $b=0.05+0.0035\ \sin(1.7434t)$. (c) Quasiperiodic state from the ordinary differential equation model described in the text. The state corresponds to a ''meandering'' spiral wave. The parameters are $\alpha_1=10/3$, $\alpha_2=-7.5$, and $\gamma_0=3.8$. (d) Effect of periodically forcing this wave: $\alpha_2=-7.5+0.6\ \sin(0.3222t)$.

(3) together with a two quadratures. We shall refer to the system described by Eqs. (3) as the reduced or s-ω system and Eqs. (1) as the full system.

To investigate the effect of parametric periodic forcing on spiral waves, we let one of the model parameters vary sinusoidally with time. Specifically we let

$$\alpha_2(t)=\alpha_2^0+A\sin(\omega_f t), \tag{4}$$

where A and ω_f are the amplitude and frequency of the forcing. The period of the forcing shall be denoted $T_f=2\pi/\omega_f$. Our approach does not require the specific case of sinusoidal forcing, but for our numerical work we shall restrict our attention to this particular case. We shall frequently be interested in the response to small amplitude forcing because this has been considered in experiments and simulations and also because scaling behavior for solutions can be obtained in the limit of weak forcing. Hence, in the following we shall frequently set $A=\epsilon$.

There is presently no established mapping between parameters in the ODE model and those of any excitable medium (experimental system or reaction-diffusion model) and hence we cannot establish a direct connection between the forcing of an excitable medium (through light variations, for example) and the forcing we choose in Eq. (4). There has been recent work in this direction [19–21]. Our concern, however, is to understand the *generic* response of waves to periodic forcing, i.e., we care about features that are independent of specific details of the medium and the forcing, and for this no rigorous connection is necessary between the

ODEs and extended excitable media. Models of real excitable systems such as the Belousov-Zhabotinsky reaction [22] are only approximate in any event and therefore it is reasonable to focus on generic properties that are common to any forced system with the symmetries of two-dimensional excitable media (rotations, reflections, and translations), whether they are spiral waves in excitable media or not.

III. FORCING OF PERIODIC WAVES

We first consider forcing in the case where the unforced dynamics are rotating waves, i.e., rigidly rotating spirals. This situation is rather well understood from the work of Davydov *et al.* [2,23], who use a kinematic approach to spiral dynamics. We consider this here because it provides a simple case for which we can illustrate our approach.

Rotating-wave solutions to the unforced full system Eqs. (1) are obtained when the reduced system Eqs. (3) has nonzero steady-state solutions, i.e., there are nonzero values s_1 and ω_1 for which $f(s_1^2,\omega_1^2)=g(s_1^2,\omega_1^2)=0$. To see that these are rotating waves for the full system, one integrates the $\dot{\phi}$ equation to obtain $\phi(t)=\omega_1 t+\phi_0$, where $\phi_0=\phi(0)$. Substituting this into the equation for $\dot{p}$ gives

$$\dot{p}=s_1 e^{i(\omega_1 t+\phi_0)}, \tag{5}$$

which in turn integrates to

$$p(t)=p_0+\frac{s_1}{i\omega_1}e^{i(\omega_1 t+\phi_0)}=p_0+R_1 e^{i(\omega_1 t+\phi_0+\delta_1)},$$

where p_0 is a constant of integration, $R_1\equiv|s_1/\omega_1|$, and $\delta_1=\mp\pi/2$ depending on the sign of ω_1. Thus we see that p traces out a circle of radius R_1 with frequency ω_1. This rotating-wave solution is stable in the full system so long as the steady state (s_1,ω_1) is stable in the s-ω subsystem.

We consider now the effect that periodic forcing has on a stable rotating wave. For this, we need solutions to the reduced system Eqs. (3) when α_2 is given by Eq. (4). We know that at least for small forcing amplitudes, the solution in the reduced system will be periodic and can be written in the form

$$s(t)=s_1+\tilde{s}(t),$$

$$\omega(t)=\omega_1+\tilde{\omega}(t),$$

where s_1 and ω_1 are the mean values of s and ω, and $\tilde{s}(t)$ and $\tilde{\omega}(t)$ are periodic with period T_f. For weak forcing, $A=\epsilon$, $\tilde{s}$ and $\tilde{\omega}$ are $O(\epsilon)$. While it is possible to obtain expressions for $\tilde{s}$ and $\tilde{\omega}$ perturbatively in powers of ϵ, these expressions are complicated and not important in detail. It is sufficient to note that when expressed in the form of Fourier series

$$\tilde{s}(t)=\sum_{k=-\infty}^{\infty}\hat{s}_k e^{ik\omega_f t},\quad \tilde{\omega}(t)=\sum_{k=-\infty}^{\infty}\hat{\omega}_k e^{ik\omega_f t},$$

the scaling of coefficients with ϵ is

$$|\hat{s}_k|,|\hat{\omega}_k|=O(\epsilon^{|k|}),\quad k\neq 0,$$

$$\hat{s}_0,\hat{\omega}_0=0.$$

As we shall show, the Fourier spectra of $\tilde{s}(t)$ and $\tilde{\omega}(t)$ are key to determining the response of rotating waves to periodic forcing. Note that the mean values of $\tilde{s}(t)$ and $\tilde{\omega}(t)$ are zero by definition, hence $\hat{s}_0=\hat{\omega}_0=0$; however, s_1 and ω_1, which are the mean values of s and ω, are modified by terms $O(\epsilon^2)$ as $\epsilon\to 0$.

To find $p(t)$ for the periodically forced system, first we integrate the equation

$$\dot{\phi}=\omega(t)=\omega_1+\tilde{\omega}(t)$$

to obtain

$$\phi(t)=\phi_0+\omega_1 t+\Omega(t),$$

where $\Omega(t)$ is defined by

$$\Omega(t)\equiv\int_0^t\tilde{\omega}(t')dt'.$$

The function $\Omega(t)$ is periodic with period T_f because $\tilde{\omega}$ has zero mean and period T_f. Substitution into the $\dot{p}$ equation gives

$$\dot{p}(t)=s(t)e^{i\phi(t)}=[s_1+\tilde{s}(t)]e^{i\Omega(t)}e^{i(\omega_1 t+\phi_0)};$$

by defining $H(t)\equiv s(t)e^{i\Omega(t)}-s_1$, this can be written

$$\dot{p}(t)=s_1 e^{i(\omega_1 t+\phi_0)}+H(t)e^{i(\omega_1 t+\phi_0)}. \tag{6}$$

The scaling of $H(t)$ is readily found by substitution of $s(t)$ and $\tilde{\omega}(t)$ into the definition of H. The result is that H is a periodic function with period T_f, which when expanded as a Fourier series

$$H(t)=\sum_{k=-\infty}^{\infty}h_k e^{ik\omega_f t} \tag{7}$$

has coefficients that scale as

$$|h_k|=O(\epsilon^{|k|}),\quad k\neq 0$$

$$|h_0|=O(\epsilon^2). \tag{8}$$

Note that the function $H(t)$ is complex.

From Eqs. (6)–(8) it follows that $\dot{p}$ has the form of the unforced expression Eq. (5) plus a perturbation that is $O(\epsilon)$. This is because the $|k|=1$ terms dominate series (7) as $\epsilon\to 0$ and this term is $O(\epsilon)$. Rewriting Eq. (6) using the Fourier expansion for $H(t)$, we have

$$\dot{p}(t)=s_1 e^{i(\omega_1 t+\phi_0)}+\sum_{k=-\infty}^{\infty}h_k e^{i[(\omega_1+k\omega_f)t+\phi_0]}. \tag{9}$$

A. Nonresonant case

There are two cases to consider. The first is the nonresonant case defined by the condition that $\omega_1+k\omega_f\neq 0$ for all k or, equivalently, that the forcing period T_f is not a multiple of the natural period $T_1=2\pi/\omega_1$. This is the ge-

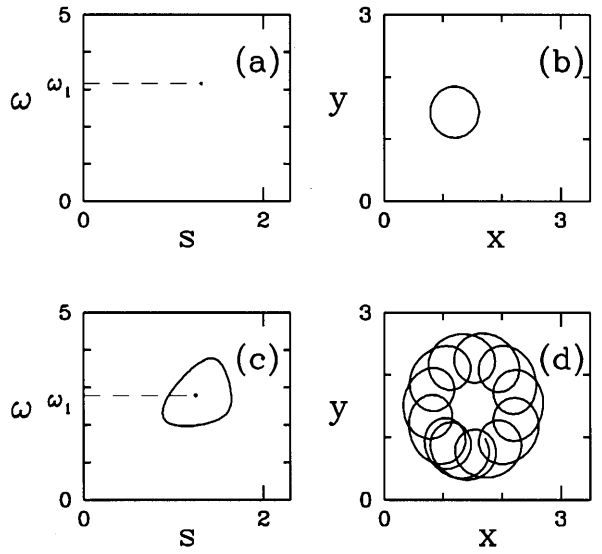

FIG. 2. Illustration of the generic case of periodic forcing of a rotating wave. Without periodic forcing, there is (a) a stable steady state in the reduced system and (b) a rotating wave in the full system shown by a plot of $p(t)$ in the complex plane. The rotation frequency ω_1 is given by the steady-state value of ω. In the case of forcing, (c) the reduced system has limit cycle and (d) the full system has a quasiperiodic solution: a modulated rotating wave. The two frequencies in this case are ω_f, the forcing frequency, and ω_1, the mean value of ω in the reduced system. As can be seen, ω_1 is shifted from the unforced value. The parameter values are $\alpha_1=10/3$, $\alpha_2=-3.5$, and $\gamma_0=3.732$, with forcing $\alpha_2=-3.5+\sin(2\pi t/2.4)$ in the lower figures.

neric situation. Then because the Fourier series is uniformly convergent we can integrate (9) term by term to find $p(t)$:

$$p(t)=p_0+R_1e^{i(\omega_1 t+\phi_0+\delta_1)}+\sum_{k=-\infty}^{\infty}\frac{h_k}{i(\omega_1+k\omega_f)}e^{i[(\omega_1+k\omega_f)t+\phi_0]}, \qquad (10)$$

where p_0, R_1, and δ_1 have the same meanings as in the unforced case.

The path $p(t)$ described by Eq. (10) is of the form of a circle given by the unforced solution plus a doubly periodic solution with frequencies ω_1 and ω_f. For any fixed, nonresonant forcing frequency, the perturbation of the circular solution goes to zero linearly with the amplitude of forcing. This is because the $|k|=1$ terms dominate the Fourier expansion (10) and this terms goes to zero linearly with forcing amplitude.

The solution given by Eq. (10) is known as a *modulated rotating wave* [24]. There is an appropriately rotating frame of reference in which the solution is seen as periodic. Such a reference frame is given by the transformation $p'=(p-p_0)e^{-i\omega_1 t}$. In this frame the dynamics are periodic with frequency ω_f. Generically the frequencies ω_1 and ω_f will be incommensurate and the dynamics described by $p(t)$ will be quasiperiodic. Figure 2 illustrates generic periodic forcing of a rotating-wave solution.

The behavior near a frequency resonance may be seen by fixing the forcing amplitude and varying the forcing frequency ω_f such that $\omega_1+k'\omega_f$ becomes small for some k'. The coefficient of the term in Eq. (10) with frequency $\Delta\equiv\omega_1+k'\omega_f$ dominates the series. In such a case we get

$$p(t)\simeq p_0+R_1e^{i(\omega_1 t+\phi_0+\delta_1)}+R_2e^{i(\Delta t+\phi_0+\delta_2)},$$

where $R_2\equiv|h_{k'}/\Delta|$ and $\delta_2\equiv\arg(h_{k'}/i\Delta)$. The path $p(t)$ is approximately the superposition of two circular motions having radii R_1 and R_2 and frequencies ω_1 and Δ, respectively. If $\omega_1/\Delta>0$, the two frequencies are of the same sign and the resulting path has the form of a flower with inward facing petals. Otherwise the frequencies are of opposite sign and the resulting flower has outward facing petals; see Fig. 3. As $\Delta\to0$, the radius R_2 diverges and we get to the case of frequency resonance.

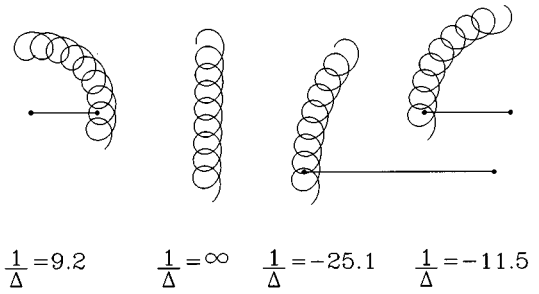

FIG. 3. Effect of periodic forcing in the vicinity of a 1-1 resonance $\omega_1-\omega_f=0$. The path $p(t)$ is plotted for four values of the forcing frequency ω_f with forcing amplitude $A=1.0$. The corresponding secondary radii R_2 are shown, except at the point of resonance $\omega_1=\omega_f=2.714$, where it is infinite. In the vicinity of the resonance, $R_2\sim1/|\Delta|$, where $\Delta=\omega_1-\omega_f$. The parameter values are $\alpha_1=10/3$, $\gamma_0=3.732$, and $\alpha_2=-3.5+A\sin(2\pi\omega_f t)$.

B. Resonant case

The resonant case is defined by the condition that $\omega_1+k'\omega_f=0$ for some k'. The series in Eq. (9) then has a secular term $h_{k'}e^{i\phi_0}$, so integrating Eq. (9) gives

$$\begin{aligned}p(t)&=p_0+R_1e^{i(\omega_1 t+\phi_0+\delta_1)}+(h_{k'}e^{i\phi_0})t+\sum_{k\neq k'}\frac{h_k}{i(\omega_1+k\omega_f)}e^{i[(\omega_1+k\omega_f)t+\phi_0]}\\&=p_0+ct+R_1e^{i(-k'\omega_f t+\phi_0+\delta_1)}+\sum_{k\neq k'}\frac{h_k}{i(k-k')\omega_f}e^{i[(k-k')\omega_f t+\phi_0]},\end{aligned}$$

where $c=h_{k'}e^{i\phi_0}$.

Thus, at resonance, in addition to the periodic part of $p(t)$, the expansion contains a term that is linear in t. The ''drift'' in position implied by this term is known as resonant drift. It has been known for almost a decade [1,2] and has now been observed in a number of different systems [7–10,25].

In the resonance case, there is a linearly translating frame of reference $p'=p-ct$, within which the state is periodic. In dynamical systems terminology such a solution is called a *modulated traveling wave*. The drift speed is given by

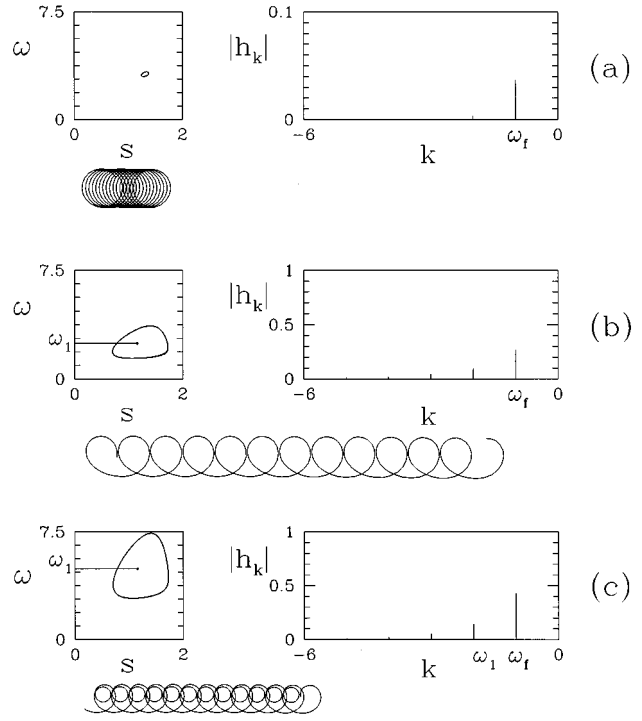

FIG. 4. Phase portraits, Fourier spectra, and paths p for different resonances. (a) Small amplitude forcing: $A=0.2$ and $T_f=1.9875$. Forcing creates a nearly elliptical orbit around the fixed point of the unforced reduced system and only the primary peak in the Fourier spectrum has significant size. In this case only the primary resonance $\omega_1=\omega_f$ produces detectable resonant drift. The parameters are $\alpha_1=10/3$, $\alpha_2=-3.5$, and $\gamma_0=3.732$. (b) Higher amplitude forcing: $A=1.2$, $T_f=2.546\,85$, and other parameters as in (a). The mean value ω_1 of the periodic orbit has changed as a result of forcing and the forcing frequency is adjusted such that $\omega_f=\omega_1$. The primary peak is much larger [note the change of scale between (a) and (b)] and the higher-order peaks in the Fourier spectrum are visible. (c) A 2:1 resonance with the parameter γ_0 changed so that $\omega_1=2\omega_f$. The parameters are as in (b), except $\gamma_0=7.363$. All paths shown are over the same time interval.

$|c|=|h_{k'}|$, which scales according to $\epsilon^{|k'|}$ as $\epsilon\to 0$. The period in the linearly translating frame is $T_f=|k'|T_1$ and the angle of the drift is determined by the coefficient $h_{k'}$ and the integration constant ϕ_0.

In Fig. 4 we show three cases of resonant forcing. For the small amplitude forcing in Fig. 4(a), the only resonance producing detectable drift is the primary resonance $\omega_1=\omega_f$, i.e., $k'=-1$. Even this drift is quite slow. The higher-harmonic peaks in the Fourier spectrum of H are very small and so drifts associated with higher-order resonances are insignificant. With the larger amplitude forcing in Fig. 4(b), the primary peak h_{-1} is larger and so the drift speed at 1:1 resonance is larger. Moreover, due to nonlinearity, the orbit in the reduced system is no longer nearly elliptical and hence higher-harmonic peaks have sufficient amplitude. Thus higher-order resonances can provide noticeable drift as is illustrated in Fig. 4(c). Note that in Fig. 4 and throughout this paper we plot the magnitude of Fourier coefficients on a linear scale.

IV. FORCING OF MODULATED ROTATING WAVES

We now consider application of periodic forcing to the case where the unforced dynamics are modulated rotating waves. These waves are quasiperiodic states that correspond to meandering spiral dynamics [14,26].

A modulated rotating wave in the unforced full system Eq. (1) is obtained when the reduced system Eq. (3) has a periodic orbit $(s(t),\omega(t))$, where s and ω are periodic with period denoted T_2. These periodic orbits arise from a supercritical Hopf bifurcation of steady-state solutions in the reduced system. The modulated rotating waves in the full system are then composed of two frequencies ω_1 and ω_2, where ω_1 is the mean value of ω and $\omega_2=2\pi/T_2$ is the frequency of the orbit in the reduced system. Near a Hopf bifurcation ω_1 will be close to the steady value of ω and ω_2 will be close to the imaginary part of the bifurcating eigenvalues. The path $p(t)$ exhibits typical behavior for meandering spiral waves in excitable media [14,16–18].

The modulated rotating waves corresponding to spiral meandering have exactly the same mathematical character as the modulated rotating waves described in Sec. III. In fact, the difference between the two cases is simply the origin of the secondary frequency. For classical two-frequency meandering waves, the secondary frequency ω_2 arises via a Hopf bifurcation, whereas in the forced rotating-wave case, the second frequency comes from forcing and is thus simply the forcing frequency ω_f. In both cases the primary frequency ω_1 has the same meaning.

A. Reduced system: A forced oscillator

We approach the study of periodically driven meandering waves by first considering periodic forcing of the periodic orbit in the reduced system and then by considering the dynamics that follows in the full systems. Figure 5 shows a phase diagram for the dynamics of the reduced system as a function of the two forcing parameters: forcing period T_f and forcing amplitude A. Paths $p(t)$ in the full system and phase portraits (s,ω) in the reduced system are shown in Fig. 6 for labeled points in the phase diagram. The parameters in the ODE model are chosen such that the unforced system has a five-petal meander pattern. This can be seen in Fig. 6(a). With high-frequency forcing the system behaves as if the driven parameter $\alpha_2=\alpha_2^0+A\sin(\omega_f t)$ were constant with its time average value α_2^0. Hence the path p and s-ω phase portrait at point (a) are indistinguishable from those of the unforced system. We shall defer consideration of the paths $p(t)$ until Sec. IV B.

The phase diagram in Fig. 5 is typical for a forced nonlinear oscillator; see, e.g., [27–30]. There are regions of frequency locking (Arnol'd tongues) within which the frequency ω_2 is rationally related to the driving frequency ω_f. These are the $p{:}q$ entrainments where $T_f/T_2=p/q$. We show only a few of the low-order entrained regions. The $p{:}q$ tongues open from $A=0$ as $A^{1/p}$, so except for the $1{:}q$ tongues, all tongues are cusps at $A=0$.

Phase portraits in Figs. 6(b)–6(d) show the dynamics of the reduced system in passing through the 1:1 tongue. The orbit in the s-ω system adjusts so that the frequency ω_2 is equal to the forcing frequency ω_f throughout this band.

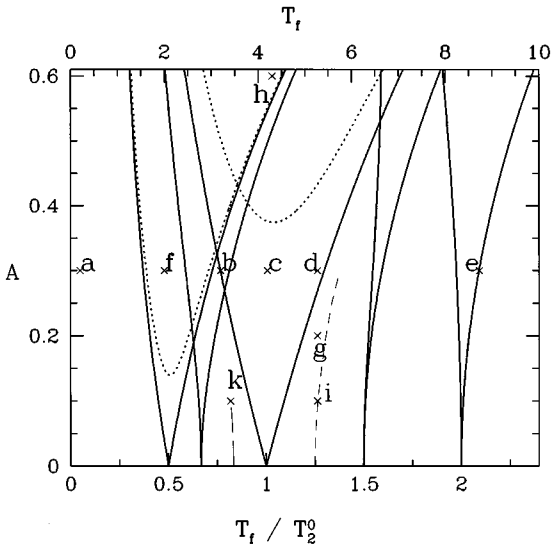

FIG. 5. Phase diagram for the ODE model as a function of forcing period T_f and forcing amplitude A. T_2^0 is the secondary period in the absence of forcing. Solid curves show the boundaries of some of the low-order entrainment tongues. Short-dashed curves are loci of period-doubling bifurcations for the 1:2 and 1:1 locked states. The period doubling in the 2:1 tongue is outside the range of the figure. Long-dashed curves are loci of the two strongest resonant drift states within the parameter range of the figure. Letters label points shown in Fig. 6 and elsewhere. The parameter values are $\alpha_1=10/3$, $\alpha_2^0=-7.5$, and $\gamma_0=3.732$.

Phase portrait (e) shows the orbit in the 2:1 tongue where $T_f/T_2=2$.

Separating regions of entrainment are curves (not shown) on which the two periods are irrationally related and the dynamics is quasiperiodic. Case (g) is effectively a quasiperiodic example, that is, it does not lie in any low-order entrainment region and is a good approximation to a trajectory on the underlying invariant torus for the reduced system.

For sufficiently large forcing amplitudes the underlying invariant torus breaks up. This is signaled by the overlap of Arnol'd tongues and by period-doubling bifurcations of the entrained states [27,31]. Once the torus has broken, one can expect chaotic states to exist as well. Points (f) and (h) illustrate the dynamics beyond the breakup of the torus. As with the quasiperiodic state, we do not know whether or not these are strictly chaotic, but they are good representations of the complex dynamics found at sufficiently large forcing amplitudes.

B. Full system: Tip paths

We now consider the form of solutions in the full system. We consider in detail only the cases where the dynamics of the reduced system is periodic (entrained) or quasiperiodic. We give a brief treatment of the chaotic case in Sec. IV C.

For either entrained or quasiperiodic states, the solution in the reduced system can be written in the form

$$s(t)=s_1+\tilde{s}(t),$$

$$\omega(t)=\omega_1+\tilde{\omega}(t),$$

where s_1 and ω_1 are the mean values of s and ω, and $\tilde{s}(t)$ and $\tilde{\omega}(t)$ are doubly periodic with periods T_2 and T_f. These two periods will be commensurate or not depending on whether the system is entrained or not. However, for the present we shall not distinguish between the two situations. Unlike in the case of rotating waves, $\tilde{s}$ and $\tilde{\omega}$ do not go to zero as the forcing amplitude goes to zero, because there is a (finite-amplitude) periodic orbit in the unforced system. Hence $\tilde{s}$ and $\tilde{\omega}$ cannot be treated as small quantities.

To find $p(t)$, we first integrate the ϕ equation to obtain

$$\phi(t)=\phi_0+\omega_1 t+\Omega(t),$$

where $\Omega(t)$ is again is defined by

$$\Omega(t)\equiv\int_0^t\tilde{\omega}(t')dt'.$$

The function Ω is doubly periodic with periods T_2 and T_f. Substitution into the $\dot{p}$ equation gives

$$\dot{p}(t)=s(t)e^{i\phi(t)}=[s_1+\tilde{s}(t)]e^{i\Omega(t)}e^{i(\omega_1 t+\phi_0)}$$

$$=s_1e^{i(\omega_1 t+\phi_0)}+Q(t)e^{i(\omega_1 t+\phi_0)},$$

where in the last equality we have defined $Q(t)\equiv s(t)e^{i\Omega(t)}-s_1$. This doubly periodic, complex function plays the same role that the periodic function $H(t)$ played in Sec. III. Here, however, $Q(t)$ is not $O(\epsilon)$.

The function $Q(t)$ can be expanded in a Fourier series as

$$Q(t)=\sum_{m,n=-\infty}^{\infty}q_{m,n}e^{i(m\omega_f+n\omega_2)t}. \tag{11}$$

Thus we have

$$\dot{p}(t)=s_1e^{i(\omega_1 t+\phi_0)}+\sum_{m,n=-\infty}^{\infty}q_{m,n}e^{i[(\omega_1+m\omega_f+n\omega_2)t+\phi_0]}. \tag{12}$$

One may now integrate this equation to obtain $p(t)$. As we shall see, there are four distinct dynamical states depending on whether or not the frequencies ω_2 and ω_f are locked and depending on whether or not there is a frequency resonance. Frequency locking is determined solely by the dynamics of the reduced system. Resonance occurs if there is a secular term in the expansion for $\dot{p}$ in Eq. (12), i.e., if there exist m',n' such that $\omega_1+m'\omega_f+n'\omega_2=0$. This is just the generalization of the resonance condition found for the forcing of rotating waves considered in Sec. III. We address separately the cases where ω_2 and ω_f are and are not frequency locked and we discuss the issue of resonance for each case. We then consider the parameter dependence and scaling of solutions.

1. Locked frequencies

Within an Arnol'd tongue the frequencies ω_2 and ω_f are rationally related, so that there exists a frequency ω_d such that $\omega_2=p\omega_d$ and $\omega_f=q\omega_d$. Thus the Fourier series can be rewritten as a sum over frequencies $k\omega_d$:

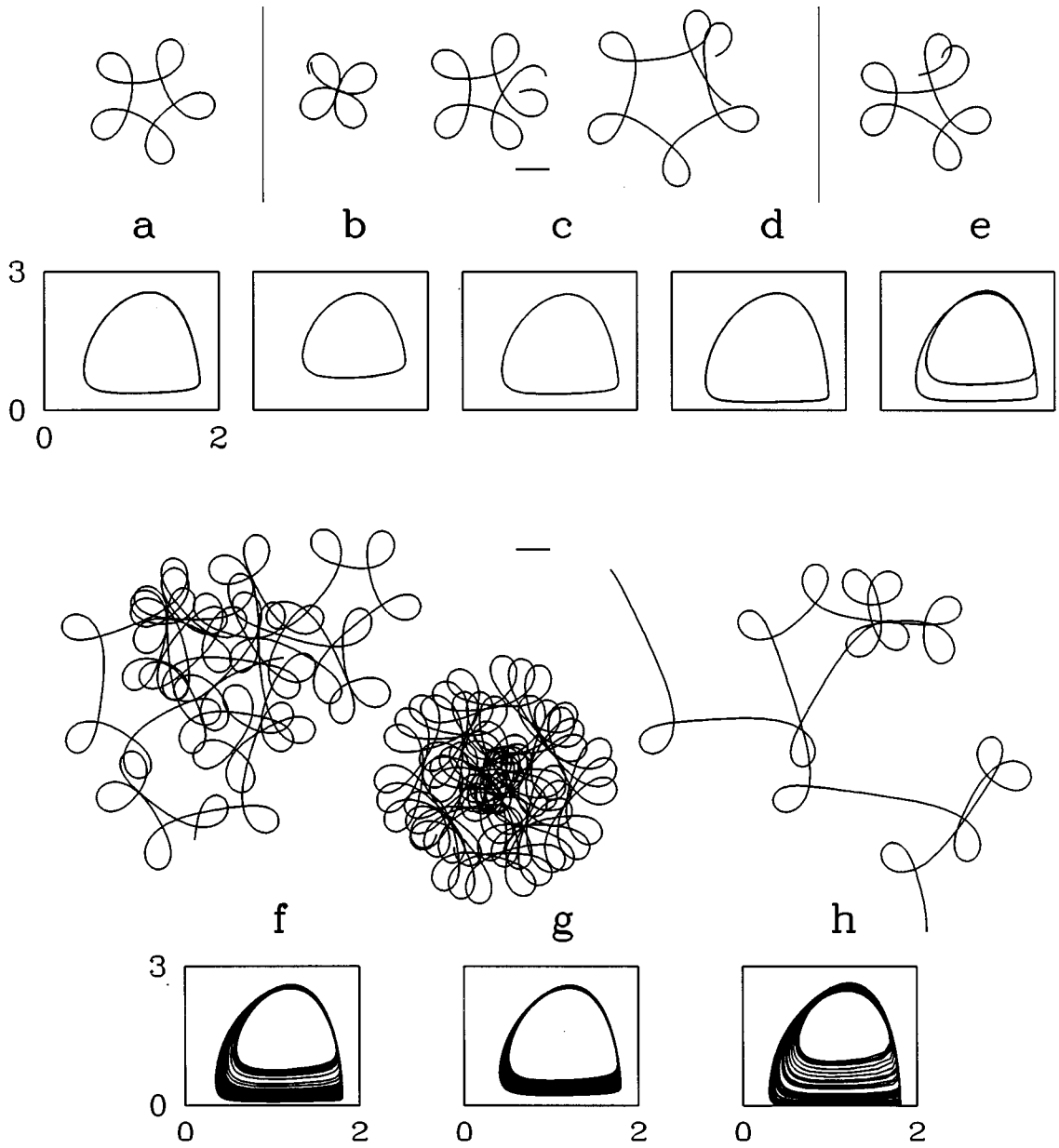

FIG. 6. Paths p for the full system and phase portraits in the reduced system at points corresponding to those labeled in Fig. 5. (a) High-frequency forcing. Here the dynamics are indistinguishable from that of the undriven system. (b)–(d) States within the 1:1 tongue. (e) State within the 2:1 tongue. (f) and (h) Chaotic orbits. (g) Quasiperiodic orbit near the 1:1 tongue. The horizontal bars show unit length in the p plane.

$$\dot{p}(t)=s_1 e^{i(\omega_1 t+\phi_0)}+\sum_{k=-\infty}^{\infty} q_k e^{i[(\omega_1+k\omega_d)t+\phi_0]}, \qquad (13)$$

and we obtain formally the same behavior for $p(t)$ as for the forcing of rotating waves (Sec. III) with ω_d playing the role of ω_f. There are only two distinct types of dynamics for $p(t)$ depending on whether or not ω_d is in resonance with ω_1. In the absence of resonance, the dynamics are quasiperiodic and the path $p(t)$ is a modulated rotating wave; in the case of resonance the path is a modulated traveling wave.

Within any given tongue, ω_d simply varies linearly with ω_f (because $\omega_f=q\omega_d$); ω_1 will also vary as a result of changes in the orbit in the reduced system under forcing. The path p is a function of both ω_1 and ω_d. When the frequencies are close to resonance the flower is large with many petals (as was illustrated in Fig. 3).

Consider the 1:1 tongue in Figs. 5 and 6(b)–6(d). The dynamics is quasiperiodic, i.e., a modulated rotating wave, along the slice through the tongue at $A=0.3$. In traversing the tongue, $\omega_d=\omega_f$ changes by about a factor of 2 and ω_1 changes by about a factor of 1.5 (this can be seen as the change in the mean value of ω in the phase portraits). The paths in Figs. 6(b)–6(d) differ from the unforced meandering wave only in the number of petals: from about four petals at the left tongue boundary where the frequency ratio is $\omega_1/\omega_f=0.756$ to just over five petals at the right tongue boundary where the frequency ratio is $\omega_1/\omega_f=0.818$.

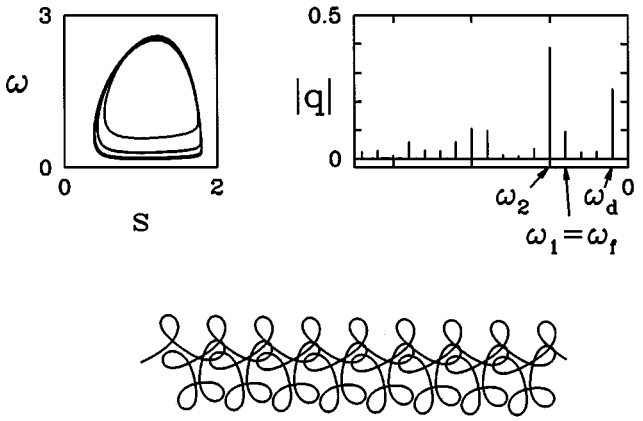

FIG. 7. Phase portrait, Fourier spectrum, and path p showing resonant drift occurring within the 5:4 entrainment tongue ($5\omega_f = 4\omega_2$). Only four of five bands are visible in the phase portrait. The path p is a modulated traveling wave. The parameters are as in Fig. 5 (with $A = 0.3$ and $T_f = 5.75$), except that $\gamma_0 = 3.692$.

Throughout the 2:1 tongue in Fig. 5 we again find only quasiperiodic dynamics. In this case, if one goes into the rotating frame $p' = (p - p_0)e^{-i\omega_1 t}$ one sees a state that is periodic with period T_f (because $q = 1$ and so $\omega_d = \omega_f$). This periodic orbit has a two-cycle (two-orbit-per-period) structure similar to that of the s-ω phase portrait in Fig. 6(e). This can be understood as arising because T_f is roughly twice as large the natural period in the reduced system.

For the parameter values of Figs. 5 and 6 we find no resonances inside any of the low-order locked tongues. However, it is possible to adjust the parameters to obtain a resonant drift inside one of the frequency-locked regions. In Fig. 7 we show a case where the value of γ_0 has been changed so that there is a resonance inside the 5:4 tongue. (The value of γ_0 affects only the frequency ω_1 and neither ω_2 nor the location of the locked tongues shown in Fig. 5.) The resonance occurs with $\omega_1 = \omega_f$, though referring to Eq. (13), the resonance is formally a 4:1 resonance between ω_d and ω_1 (in the 5:4 tongue, $\omega_f = 4\omega_d$ so $\omega_1 = 4\omega_d$). The resonant drift shown in Fig. 7 is a modulated traveling wave that thus can be seen as periodic in a comoving reference frame.

2. Unlocked frequencies

In the quasiperiodic regime, outside the Arnol'd tongues, different types of behavior are obtained. Again there are two cases corresponding to whether or not there is a resonance between ω_1 and the other two frequencies in the problem: ω_f and ω_2.

In the nonresonant case, $\omega_1 + m\omega_f + n\omega_2 \neq 0$ for all n, m, we may integrate Eq. (12) to obtain

$$p(t) = p_0 + R_1 e^{i(\omega_1 t + \phi_0 + \delta_1)} + \sum_{m,n=-\infty}^{\infty} \frac{q_{m,n}}{i(\omega_1 + m\omega_f + n\omega_2)} e^{i[(\omega_1 + m\omega_f + n\omega_2)t + \phi_0]}.$$

Thus $p(t)$ contains three independent frequencies ω_1, ω_2, and ω_f. This is mathematically the same as the hypermeander found in unforced spiral systems [17,32]. In the rotating frame of reference $p' = (p - p_0)e^{-i\omega_1 t}$ the dynamics is quasiperiodic with two frequencies ω_f and ω_2. Figure 8 shows such a situation.

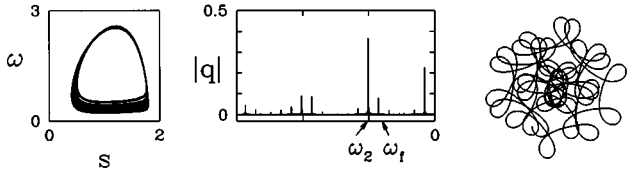

FIG. 8. Phase portrait, Fourier spectrum, and path p for a typical three-frequency quasiperiodic orbit. The phase portrait depicts the dense winding on a torus with two frequencies ω_2 and ω_f that are not rationally related. The Fourier spectrum contains peaks at ω_2, ω_f and all sum and difference frequencies. The path $p(t)$ consists of three independent frequencies ω_1, ω_2, and ω_f and after sufficient time it would densely fill a region in the p plane. The parameter values are $\alpha_1 = 10/3$, $\alpha_2 = -7.5$, $\gamma_0 = 3.732$, $A = 0.3$, and $T_f = 6.3$, corresponding to point (g) in Fig. 5.

In the resonant case there exist n' and m' such that $\omega_1 + m'\omega_f + n'\omega_2 = 0$, and so there is a secular term in Eq. (12) given by $q_{m',n'}e^{i\phi_0}$. Thus integration gives

$$p(t) = p_0 + R_1 e^{i(\omega_1 t + \phi_0 + \delta_1)} + (q_{m',n'}e^{i\phi_0})t + \sum_{m,n \neq m',n'} \frac{q_{m,n}}{i(\omega_1 + m\omega_f + n\omega_2)} e^{i[(\omega_1 + m\omega_f + n\omega_2)t + \phi_0]},$$

or, using the condition for resonance $\omega_1 = -m'\omega_f - n'\omega_2$ and defining $c = q_{m',n'}e^{i\phi_0}$,

$$p(t) = p_0 + R_1 e^{i[(-m'\omega_f - n'\omega_2)t + \phi_0 + \delta_1]} + ct + \sum_{m,n \neq m',n'} \frac{q_{m,n}}{i[(m-m')\omega_f + (n-n')\omega_2]} \times e^{i\{[(m-m')\omega_f + (n-n')\omega_2]t + \phi_0\}}.$$

Thus we again find drift in the case of a frequency resonance. There is a translating frame of reference $p' = p - ct$ in which the path is quasiperiodic with the two frequencies ω_f and ω_2.

In Fig. 9 we show three examples of resonant drift for nonentrained states that is drift states that do not occur in any low-order locking. In the first, Fig. 9(a), $\omega_1 = \omega_f$, i.e., $m' = -1$ and $n' = 0$. The translation speed of the path p is given by the coefficient $q_{1,0}$ corresponding to the peak at frequency $\omega_1 = \omega_f$. This strong resonance is the simplest possible and has been seen experimentally [7,9]. However, an almost equally fast drift occurs for the case $\omega_1 = 2\omega_2 - \omega_f$, i.e., $m' = 1$ and $n' = -2$. The nonlinear interaction between natural frequency ω_2 and the driving frequency ω_f is such as to produce a significant peak in the Fourier spectrum at $2\omega_2 - \omega_f$. When this peak coincides with ω_1 a strong drift occurs. For the third example we show the resonance $\omega_1 = 4\omega_f$ that lies outside the phase diagram of Fig. 5.

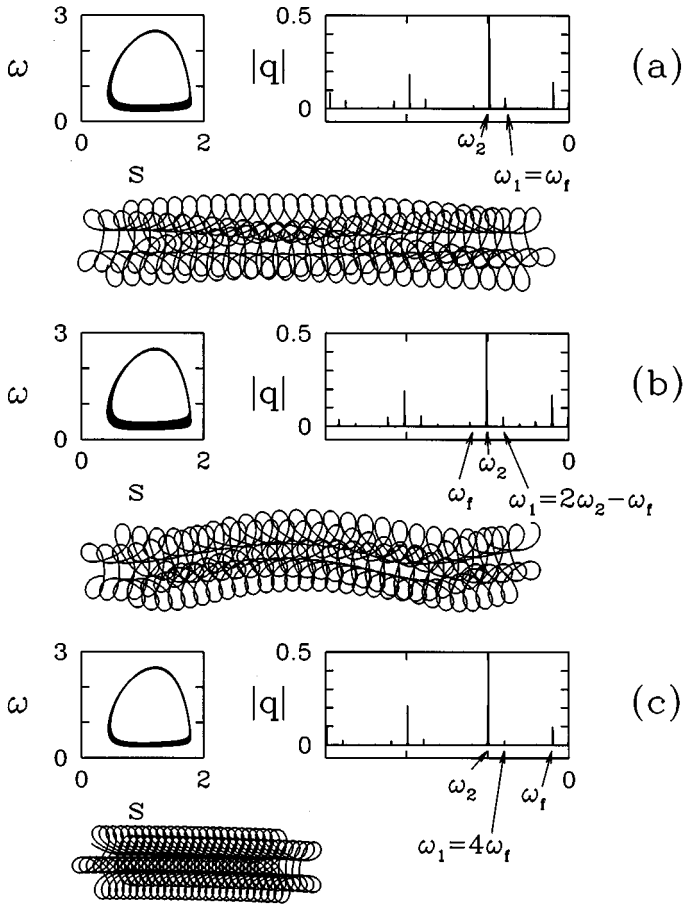

FIG. 9. Phase portraits, Fourier spectra, and paths p illustrating various resonant drift states. (a) $\omega_f=\omega_1=2\pi/5.27$, corresponding to point i in Fig. 5; (b) $\omega_f=2\omega_2-\omega_1=2\pi/3.407$, corresponding to point k in Fig. 5; (c) $\omega_f=\omega_1/4=2\pi/20.84$, which is outside the parameter range in Fig. 5. The amplitude of the forcing is the same, $A=0.1$, in all cases. The drift speed is given by the size of the peak in the Fourier spectrum at ω_1.

3. Parameter dependence of resonant drifts

For fixed model parameters one would like to know the location of resonant drifts as a function of forcing amplitude and forcing period, i.e., the location of drifts on the phase diagram in Fig. 5. This is greatly complicated by the phenomenon of the frequency locking. The location and size of peaks in the Fourier spectrum of $Q(t)$ are nonsmooth functions of forcing amplitude and period, and also ω_1 varies nonsmoothly as a function of these. For small forcing amplitudes, however, the nonsmooth dependence of the various quantities is not significant in practice, and the loci of drift states can be well approximated by a set of smooth curves in parameter space. This is illustrated by the two curves in Fig. 5.

Drift states originate from the $A=0$ axis at all points such that $\omega_1+m'\omega_f+n'\omega_2=0$ for some m',n'. Of these only a few will be sufficiently strong to be detected in experiment or in numerical simulations of reaction-diffusion models. We have illustrated some of the more important examples in Figs. 5 and 9. Which drifts will be strongest depends on the nonlinear interaction between ω_2 and ω_f as well as on the value of ω_1. Hence, while the ODE model can be used to determine generally the important resonances, it cannot be used to predict exactly which drifts will be strongest in any particular experiment. In the ODE model it is not difficult to find resonances for most combinations of small m' and n'.

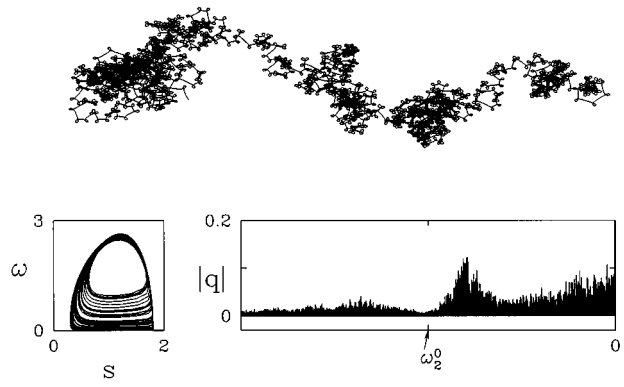

FIG. 10. Path p, phase portrait, and Fourier spectrum of a chaotic state. The broadband Fourier spectrum results in an irregular tip path. Parameters correspond to point h in Fig. 5.

We note that outside the entrainments, resonant drift states should be generic. This is because in the unlocked case, ω_2/ω_f is irrational and hence the Fourier spectrum has peaks on a dense set of frequencies $(m\omega_f+n\omega_2)$. Therefore the condition that $\omega_1+m'\omega_f+n'\omega_2=0$ for some m', n' can be expected to hold generically outside of the tongues. This implies that at low forcing amplitude, where the unlocked states have almost full measure, resonant-drift states should abound. While true, this is not important in practice, for as we have said, at low forcing amplitudes only a few peaks in the Fourier spectrum are of significant size.

C. Chaotic states

For completeness we consider briefly the case of a chaotic state beyond the breakup of the torus in the reduced system. We may formally proceed exactly as in the preceding subsection, but the Fourier spectra are no longer guaranteed to converge in the long-time limit. For this reason we limit ourselves to numerical examples. The Fourier spectra we have examined at the points labeled (f) and (h) in Fig. 5 seem to converge, but only after many thousands of primary rotation periods T_1. Figure 10 shows our results for the chaotic state corresponding to point (h). The Fourier spectrum is quite broadband, showing significant amplitudes at all frequencies up to approximately ω_2^0, the secondary frequency of the unforced system. There is a broad main peak in the vicinity of, though slightly below, ω_2^0. The path p ''randomly'' jumps between a regular and drifting flower pattern.

V. DISCUSSION

A. Summary of results

We begin with a brief synopsis of our method and results. The key to our dynamical-systems based approach has been to understand the role of symmetry in the problem and in particular to separate the symmetry variables associated with Euclidean symmetry (position $p=x+iy$ and phase angle

ϕ) from the remainder of the nonlinear system (the reduced system). In making this separation we obtain a very simple and broadly applicable treatment of the forcing problem which can be summarized in two parts.

(a) Reduced system. We first consider the dynamics of the problem in the reduced system. For the particular model equations studied, this means considering a forced two-variable dynamical system. The dynamics of such a system are quite well understood. In the absence of forcing, only two types of states are possible: steady states and limit cycles (corresponding to rigidly rotating and meandering spirals, respectively). In the first case, with forcing, the dynamics of the reduced system are then those of a driven damped oscillator (the steady state is a stable focus); in the later case with forcing one obtains a classical frequency-locking picture as a function of forcing amplitude and forcing period. We emphasize that the frequency entrainments are associated with the reduced system and are completely decoupled from the symmetry variables. The Fourier spectra of the variables in the reduced system then play a key role in determining the dynamics of the full system.

(b) Full system. The dynamics of the full system, in particular the behavior of the path $p(t)=x(t)+iy(t)$, can be found from the dynamics of the reduced system by simple quadrature. One can formally integrate the equation for the phase angle $\dot{\phi}=\omega$ and from this obtain an expression for $\dot{p}(t)$ in the form of a Fourier series. The Fourier spectrum contains peaks at frequencies $\omega_1+\omega_j$, where ω_j represents any of the frequencies found in the spectra of variables in the reduced system. This may be a discrete or continuous set depending on the dynamics of the reduced system. The frequency ω_1 is the mean value of $\omega(t)$ from the reduced system and it enters the dynamics of the full system through the integration of the equation for the phase angle. The full system exhibits resonant drift if there is a frequency ω_j in the reduced system such that $\omega_1+\omega_j=0$. The coefficient of the corresponding term in the Fourier spectrum of $\dot{p}$ gives the speed of this drift. There is then a translating frame of reference in which the dynamics of the full system is of the same type as in the reduced system. There is no resonant drift if $\omega_1+\omega_j\neq 0$ for all frequencies ω_j. In this case there is a rotating frame (with frequency ω_1) within which the dynamics is like that of the reduced system.

We stress that the above approach is general and does not depend on the particular form of dynamics in the reduced system. The ODE system that we have examined is just a low-order expansion for the dynamics of meandering spirals and thus is the most basic system describing forced meandering waves. Our approach and intuition are nevertheless fully applicable to higher-dimensional dynamics in the reduced system. Whatever model one takes for spiral dynamics on the infinite plane, it will necessarily be invariant under some representation of Euclidean symmetry and one can obtain a reduced system by considering the full system modulo these symmetries. The condition for resonance drift then follows in exactly the way we have considered here.

B. Comparison with other work

Davydov *et al.* [2] provided an initial mathematical treatment of resonant drift for rigidly rotating spiral waves under homogeneous periodic forcing. Their approach was based on a kinematic model of spiral dynamics in which one disregards the thickness of the excited area and models the spiral as a one-dimensional curve. This approach is nicely reviewed in [33]. From their approach, Davydov *et al.* obtained the important features of rigidly rotating spiral waves under periodic forcing. Specifically they discovered resonant drift and found the applicable scaling laws: at a 1:k resonance the drift speed scales as $A^{|k|}$ for forcing amplitude A and near resonance the radius of the secondary motion is proportional to the reciprocal of the frequency difference. Moreover, in their approach the drift speed is related to properties of the medium and so one has the ability, in some cases, to obtain not only the qualitative form of the scaling laws but also quantitative information about the drift speed.

Our work not only confirms the scaling laws but also shows clearly that these scaling laws depend only on the symmetries of the system (something that has also been noted in [5]). The scaling follows from the periodic forcing of a rotating wave in the plane at a resonant frequency. In no way does it matter that the system considered is an excitable medium or that the rotating wave is a spiral wave. In this sense our results are much more general that those of Davydov *et al.* because their approach is based on the case of a weakly excitable media. Our approach applies to any physical system. Resonant drift for rigidly rotating spirals has been confirmed in numerous experiments and numerical simulations [7–10,25].

There have been several recent studies of periodic forcing of meandering spiral waves using the light-sensitive Belousov-Zhabotinsky reaction (Schrader *et al.* [7,8]; Zykov *et al.* [9,10]). Resonant-drift-like behavior has been observed both in experiments and simulations at specific forcing frequencies. Zykov *et al.* [9] have found quasiperiodic drift for forcing with $T_f=T_1$, i.e., forcing at the primary spiral period. As we have seen, this is expected to lead to the fastest spiral drift. They have also found a drift with low-frequency forcing, which they refer to as ''secondary'' resonant drift. In fact, it would appear that what they observe is simply a high-order (4:1) resonance between T_f and T_1. We note that resonant drifts occur for $T_f=kT_1$ for any k and so this secondary resonant drift is just one of many possible cases.

Schrader *et al.* have also observed resonance drift of meandering waves in an Oregonator model. In particular, they have found a frequency-locked resonant drift for $T_f=T_1$ (the entrainment is apparently within the $T_f:T_2=4:3$ entrainment tongue) [34].

We believe that our analysis makes clear which frequency interactions give rise to drift in the meandering case, and we are able to predict where in parameter space drifts will occur. As far as we are aware, no one has found or sought any of the more complex resonances such as those we show in Fig. 9(b). It should be possible to find such a resonance either in experiment or in numerical simulations of a reaction-diffusion model.

Frequency locking in the case of forced meandering waves was initially described by Zykov *et al.* [10] and then by Schrader *et al.* [7]. The experimental parameters for the Zykov work were such as to give a five-petal meander flower for the unforced system and this motivated our choice of ODE parameters for this work. With forcing they find evi-

dence of 1:2, 1:1, and 2:1 entrainments. Schrader *et al.* show evidence of 1:1, 3:2, and 2:1 entrainments. Zykov *et al.* also show an Arnol'd tongue diagram from numerical studies of an Oregonator model. This diagram is quite similar to that shown in Fig. 5 from the ODE model.

An interesting point is that in the numerical study of Zykov *et al.* [9], the primary frequency is affected only slightly by the forcing amplitude. This is evidenced by the fact that the frequency of primary resonance is essentially independent of forcing amplitude. On the contrary, in the ODE system the primary frequency varies considerably with forcing amplitude and forcing frequency. Schrader *et al.* [7] also find that the primary frequency can change considerably with forcing period.

C. Future work

We conclude by noting some areas for future work. As stated in the Introduction, a large part of the motivation for this work has been the belief that it might some day be possible to use resonant drift as a means of low-voltage cardiac defibrillation. If this is so, then a clear theoretical understanding of periodic forcing is necessary for spiral waves to be predictable in the presence of inhomogeneities, anisotropies, and lateral boundaries. Biktashev and Holden [5] have made progress in understanding the interactions of drifting spirals with boundaries, but further work is necessary to understand fully the dynamics of forced spiral waves in a system with the spatial structure of heart tissue. Most importantly, one needs to understand the periodic forcing of waves in three space dimensions [26,35]. The waves of electrical activity in the heart are truly three dimensional and one must properly address periodic forcing in this case if one is to have useful theoretical understanding of cardiac defibrillation. We believe that the dynamical-systems based approach that we have adopted can be extended to these more complicated situations.

Several researchers have looked into feedback mechanisms to control spiral waves. Biktashev and Holden [6], for example, use feedback to overcome the effect of medium boundaries in resonant drift. Grill *et al.* [36] have applied feedback controlled forcing to obtain stable meandering patterns. It should be a relatively simple matter to incorporate feedback into our ODE approach.

The other area in which it would be important to extend our results is in the direction of bifurcation theory. There are many aspects of this work that are interesting mathematically but we have not addressed with mathematical rigor. It would be interesting, for example, to consider the interaction of periodic forcing with the Hopf bifurcation from rotating to modulated rotating waves. Periodic forcing at a Hopf bifurcation point is an interesting mathematical situation [28,29], and the additional interplay with the symmetries of spiral waves is worth exploring. Also worth consideration is the case where the reduced dynamics are more complicated than periodic, for it is known that spiral waves in excitable media exhibit quite complex dynamics in the reduced system [17,32]. Finally, there has been recent work using ''spiral boundary conditions'' to generate rotating waves in simple one-component chemical reactions [37]. It would be quite interesting to apply periodic forcing to such a system.

ACKNOWLEDGMENTS

We wish to thank V. Biktashev for helpful discussions and L. S. Tuckerman for her suggestions. This work has been supported in part by a grant from the Royal Society.

[1] K. Agladze, V. Davydov, and A. Mikhailov, Pis'ma Zh. Éksp. Teor. Fiz. **45**, 601 (1987) [JETP Lett. **45**, 767 (1987)].
[2] V. Davydov, V. Zykov, and A. Mikhailov, Usp. Fiz. Nauk **161**, 45 (1991) [Sov. Phys. Usp. **34**, 665 (1991)].
[3] V. Biktashev and A. Holden, Phys. Lett. A **181**, 216 (1993).
[4] V. Biktashev and A. Holden, J. Theor. Biol. **169**, 101 (1994).
[5] V. Biktashev and A. Holden, Chaos Solitons Fractals **5**, 575 (1995).
[6] V. Biktashev and A. Holden, Proc. R. Soc. London Ser. B **260**, 211 (1995).
[7] A. Schrader, M. Braune, and H. Engel, Phys. Rev. E **52**, 98 (1995).
[8] M. Braune, A. Schrader, and H. Engel, Chem. Phys. Lett. **222**, 358 (1994).
[9] V. Zykov, O. Steinbock, and S. C. Müller, CHAOS **4**, 509 (1994).
[10] O. Steinbock, V. Zykov, and S. Müller, Nature **366**, 322 (1993).
[11] D. Barkley, Physica D **49**, 61 (1991).
[12] D. Barkley, Phys. Rev. Lett. **72**, 164 (1994).
[13] D. Barkley and I. Kevrekidis, CHAOS **4**, 453 (1994).
[14] D. Barkley, in *Chemical Waves and Patterns*, edited by R. Kapral and K. Showalter (Kluwer, Dordrecht, 1995), pp. 163–189.
[15] The role of the variables and parameters is identical to the previous treatment. Here the variable w does not appear and the equations are written directly using the variable $\omega = \gamma_0 w$.
[16] D. Barkley, Phys. Rev. Lett. **68**, 2090 (1992).
[17] A. Winfree, CHAOS **1**, 303 (1991).
[18] Z. Nagy-Ungvarai, J. Ungvarai, and S. Müller, CHAOS **3**, 15 (1993).
[19] C. Wulff, Dissertation thesis, Freie Universität Berlin, 1996 (unpublished).
[20] V. N. Biktashev, A. V. Holden, and E. V. Nikolaev, Int. J. Bifurc. Chaos (to be published).
[21] M. Golubitsky, V. G. LeBlanc, and I. Melbourne (unpublished).
[22] R. Field and R. Noyes, J. Chem. Phys. **60**, 1877 (1974).
[23] A. Mikhailov and V. Zykov, Physica D **52**, 379 (1991).
[24] D. A. Rand, Arch. Rat. Mech. Anal. **79**, 1 (1982).
[25] S. Nettesheim, A. von Oertzen, H. Rotermund, and G. Ertl, J. Chem. Phys. **98**, 9977 (1993).
[26] A. Winfree, *When Time Breaks Down* (Princeton University Press, Princeton, 1987).
[27] V. Arnol'd, *Geometrical Methods in the Theory of Ordinary-Differential Equations* (Springer, New York, 1983).
[28] J. Gambaudo, J. Diff. Eq. **57**, 172 (1985).

[29] W. Vance, G. Tsarouhas, and J. Ross, Prog. Theor. Phys. Suppl. **99**, 331 (1989).
[30] K. Krischer, M. Eiswirth, and G. Ertl, J. Chem. Phys. **97**, 307 (1992).
[31] D. Aronsen, M. Chory, G. Hall, and R. McGhee, Commun. Math. Phys. **83**, 303 (1982).
[32] T. Plesser and K. Muller, Int. J. Bifur. Chaos **5**, 1071 (1995).
[33] A. Mikhailov, V. Davydov, and V. Zykov, Physica D **70**, 1 (1994).
[34] In [7] T_{mod} is the forcing period that we call T_f and T_{loop} is the secondary period that we call T_2. Schrader *et al.* also observe a resonant drift with $T_f = 2T_1$.
[35] A. Mikhailov, Chaos Solitons Fractals **5**, 673 (1995).
[36] S. Grill, V. Zykov, and S. Müller, Phys. Rev. Lett. **75**, 3368 (1995).
[37] M. Dellnitz, M. Golubitzky, A. Hohmann, and I. Stewart, Int. J. Bifur. Chaos **5**, 1487 (1995).